Citation: Molecular Therapy–Nucleic Acids (2013) 2, e82; doi:10.1038/mtna.2013.10

www.nature.com/mtna

Voltage Preconditioning Allows Modulated Gene Expression in Neurons Using PEI-complexed siRNA

Arati Sridharan, Chetan Patel and Jit Muthuswamy

We present here a high efficiency, high viability siRNA-delivery method using a voltage-controlled chemical transfection strategy to achieve modulated delivery of polyethylenimine (PEI) complexed with siRNA in an *in vitro* culture of neuro2A cells and neurons. Low voltage pulses were applied to adherent cells before the administration of PEI-siRNA complexes. Live assays of neuro2a cells transfected with fluorescently tagged siRNA showed an increase in transfection efficiency from 62 ± 14% to 98 ± 3.8% (after −1 V). In primary hippocampal neurons, transfection efficiencies were increased from 30 ± 18% to 76 ± 18% (after −1 V). Negligible or low-level transfection was observed after preconditioning at higher voltages, suggesting an inverse relationship with applied voltage. Experiments with propidium iodide ruled out the role of electroporation in the transfection of siRNAs suggesting an alternate electro-endocytotic mechanism. In addition, image analysis of preconditioned and transfected cells demonstrates siRNA uptake and loading that is tuned to preconditioning voltage levels. There is approximately a fourfold increase in siRNA loading after preconditioning at −1 V compared with the same at ±2–3 V. Modulated gene expression is demonstrated in a functional knockdown of glyceraldehyde 3-phosphate dehydrogenase (GAPDH) in neuro2A cells using siRNA. Cell density and dendritic morphological changes are also demonstrated in modulated knockdown of brain derived neurotrophic factor (BDNF) in primary hippocampal neurons. The method reported here has potential applications in the development of high-throughput screening systems for large libraries of siRNA molecules involving difficult-to-transfect cells like neurons.

Molecular Therapy–Nucleic Acids (2013) **2**, e82; doi:10.1038/mtna.2013.10; published online 26 March 2013
Subject Category: siRNAs, shRNAs, and miRNAs Gene Vectors

Introduction

We present here a novel method for voltage-controlled delivery of siRNA to neuro2a cells and primary hippocampal neurons that is tuned to the level of preconditioning voltage applied to the cells. Non-viral transfection methods are increasingly used in both *in vitro* and *in vivo* systems for siRNA delivery.[1] However, they have mixed results in difficult-to-transfect cells such as murine neuroblastoma cells of the neuro2a cell line and primary neuronal cells, where chemical transfection typically yields 3–30% efficiency.[2–4] This is in part due to cell size, variations in cell shape, and stage in the cell cycle.[5] Although multiple alternate transfection systems have made major strides, all have significant trade-off issues between transfection efficiency and viability.[6] As neuro2a cells are used in current high-throughput assays for molecular therapy, methods to improve and control the transfection efficiency, especially under small sample size conditions, have tremendous potential.

Polyplex nanoparticle vectors like polyethylenimine (PEI) are widely used as transfection agents and have shown significant promise *in vivo*.[7,8] Typical polymer based transfection efficiencies of 15–20% have been reported for siRNA delivery.[9] With chemical modifications the efficiencies can increase to 60–80%.[10–12] Recent studies have reported optimized efficiencies of upto 60–80% using PEI (branched 25 kDa) and Lipofectamine 2000 for siRNA delivery in neuro2a.[8] Although alternate nanoparticle carrier systems like gold, metal hydroxide, and double layer hydroxide based nanoparticle carriers have reported high efficiencies for siRNA in cortical neurons, inconsistencies in transfection efficiency (6–80%) among samples persist.[13,14] In addition to biological variability, high variability of siRNA based silencing between individual or small populations of cells still remains a significant issue when using chemical transfection agents.[15–17] PEI-based systems, similar to other commercial agents, use cationic polymers to form nanoparticle complexes (~80–150 nm) with siRNA.[18] PEI/siRNA nanocomplexes bind to the membrane via electrostatic interactions and rely on multiple, natural, endocytotic pathways for internalization into the cell.[19] Branched PEI (*i.e.,* 25 kDa)-based systems are hypothesized to be highly effective because of their ability to escape the endosomal pathway via the proton "sponge" effect.[20–22] The reliance on a passive, electrostatic interaction to facilitate transfection often requires high confluency (>70% for neuro2a) and long incubation times (upto 5 hours) without the presence of serum. This increases the susceptibility to cell death and significant perturbations in cell homeostasis, leading to variability in gene silencing. This effect may be compounded when evaluating small cell populations in high-throughput systems. As we move into the next generation of transfection methodology for high-throughput platforms, it is critical to achieve consistent, high transfection efficiency while preserving cell viability in small samples of cell populations.

In this study, a voltage-controlled, PEI-based transfection method with high efficiency is presented where the uptake is tuned to the level of preconditioning voltage. The majority of electric field–assisted transfection reported in the past involves electroporation, where high electric field intensities (0.5–10 kV/cm) are applied to reversibly permeabilize the membrane and allow naked siRNA or DNA into the cell. Large-scale, high-voltage electroporation typically yields 20–30%

School of Biological & Health Systems Engineering, Ira A. Fulton School of Engineering, Arizona State University, Tempe, Arizona, USA. Correspondence: Jit Muthuswamy, SBHSE, ECG 335, P.O. Box 879709, Arizona State University, Tempe, AZ 85287–9709, USA . E-mail: jit@asu.edu
Keywords: controlled dosage; electrical preconditioning; primary neurons; siRNA; tunable transfection
Received 30 July 2012; accepted 30 January 2013; advance online publication 26 March 2013. doi:10.1038/mtna.2013.10

efficiency with a large decrease in viability.[23,24] With optimization of high-voltage pulse regimen and proprietary electroporation buffers, >95% transfection efficiency in primary neurons has been demonstrated by individual groups.[23] A recent optimization study of electroporation parameters reported high siRNA transfection efficiencies upto 75% *in vitro*[25] for neuro2a cells. Also, low voltage methods like microscale electroporation allow for rapid, localized, site-specific delivery for small sample sizes while preserving viabilities of 82% in adherent cells *in vitro*.[6,26–30] Nanochannel electroporation–based systems have also been shown to achieve high transfection efficiencies in Jurkat cells with a 10–12% variation in dosing levels, though currently, it remains a labor-intensive and low-throughput process requiring precise alignment of nonadherent cells and the nanochannels.[31] Previous literature on combining electroporation with chemical transfection show detrimental effects on the transfection efficiency when compared with either method alone.[32,33] However, enhancement in transfection efficiency has been observed in other electric field–assisted methods where low voltage dc or pulse trains of voltages (~300 V/cm) or currents (<500 μA) are used to electrophoretically guide nanoparticle-loaded siRNA *in vivo*.[34,35] The above method has shown improvements in viability and transfection efficiency via electrophoretic coupling.[36–38] Therefore, electric field–assisted methods, in general, are characterized by advantages such as their ability to achieve transfection in targeted cells and rapid delivery protocol. In this report, we take advantage of the tunability of electric field–based systems to develop a hybrid transfection method that is a distinct alternative to both electroporation and electrophoretic coupling based methods reported above.

In this report, we use extremely low voltage pulse trains (<3 V/mm or 30 V/cm) to precondition adherent neuro2a cells and primary hippocampal neurons before their exposure to PEI-siRNA complexes and demonstrate successful voltage-controlled modulation of the uptake of these complexes by the cells. A high transfection efficiency (~90% and ~76% for neuro2a and primary neurons respectively) at −1 V and low transfection efficiencies at higher voltages (>2 V) were observed. For the sake of clarity, we measure siRNA "uptake" in the cells by the fraction of the pixels inside the cell that are fluorescent (due to the Alexa-555 conjugated siRNA). We measure siRNA "loading" in the cells by the mean pixel intensity weighted by the fraction of pixels at each intensity level inside the cell. Therefore, the siRNA uptake metric quantitatively reflects the spatial spread of siRNA within the cell and siRNA loading metric quantitatively captures both the spatial spread and dosage of siRNA within the cell. siRNA loading in cells increased approximately threefold between the low and high voltages. Analysis of individual cells at different preconditioning voltages suggested lower siRNA loading in the intracellular space at high voltages. Finally, functional silencing was demonstrated using glyceraldehyde 3-phosphate dehydrogenase (GAPDH) siRNA in neuro2a cells and brain derived neurotrophic factor (BDNF) siRNA in primary hippocampal neurons that was correlated to the level of preconditioning voltage applied. Consistent, rapid, and efficient delivery of siRNAs using the reported technique in difficult-to-transfect cells has significant applications in high-throughput technologies.

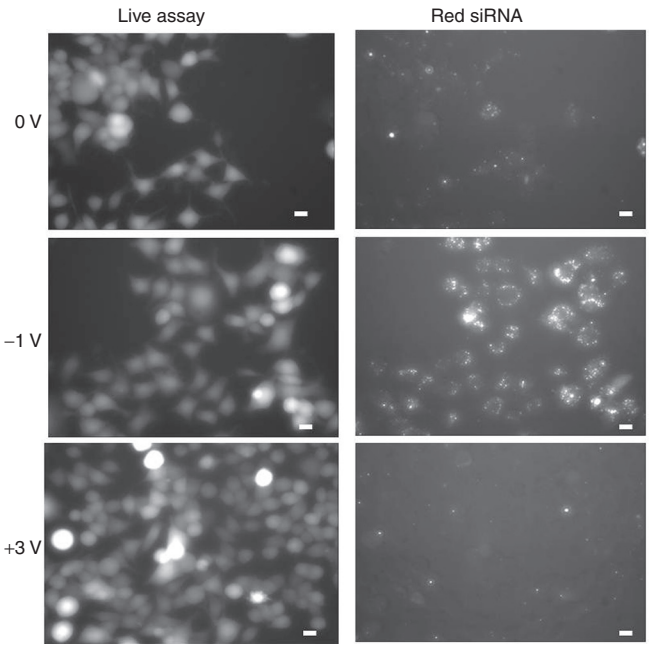

Figure 1 Voltage-modulated transfection of neuro2a cells with Alexa-555 conjugated negative control siRNA (Invitrogen). A standard live assay with calcein AM was conducted on transfected neuro2a cells preconditioned with different voltages. Transfection efficiencies were 62 ± 14% (0 V), 98 ± 3.8% (−1 V), and 37 ± 7.5% (+3 V). The distribution of fluorescent intensities after preconditioning with −1 V was more uniform throughout the cell compared with those at 0 or 3 V, suggesting higher cellular uptake at −1 V. Scale bar represents 50 μm.

Results

Transfection efficiencies of PEI-siRNA complexes with voltage preconditioning

Fluorescently tagged siRNA were complexed with PEI and administered to neuro2a cells that were preconditioned at different voltages. A live cell assay was performed on transfected cells 8 hours after the application and removal of 0 V, −1 V, and +3 V (**Figure 1**). Under no voltage conditions (0 V), siRNA transfection efficiencies were 62 ± 14% in live cells. There was a significant increase in siRNA transfection efficiencies to 98 ± 3.8% after the application and removal of −1 V. After preconditioning the cells at 3 V, 37 ± 7.5% of the live cells were visibly transfected, however with much less fluorescent intensity in the transfected cells compared with those after preconditioning at −1 V. Similar modulation trends were also observed in siRNA uptake in primary hippocampal neurons. In primary hippocampal neurons (DIV4) transfection efficiency with PEI/siRNA complexes were 76 ± 10% assessed 18 hours after preconditioning with −1 V compared with 30 ± 18% with no preconditioning (0 V) as shown in **Figure 2**. Virtually no fluorescently tagged siRNA was observed to enter neurons preconditioned at +3 V. Images of primary neurons that were preconditioned showed no difference in morphology compared with the non-preconditioned neurons. Morphologically, **Figure 2a** and **Figure 2b** show the live assay and fluorescently tagged scrambled siRNA uptake respectively. **Figure 2c** shows a close up of overlapped live and red images of transfected neurons.

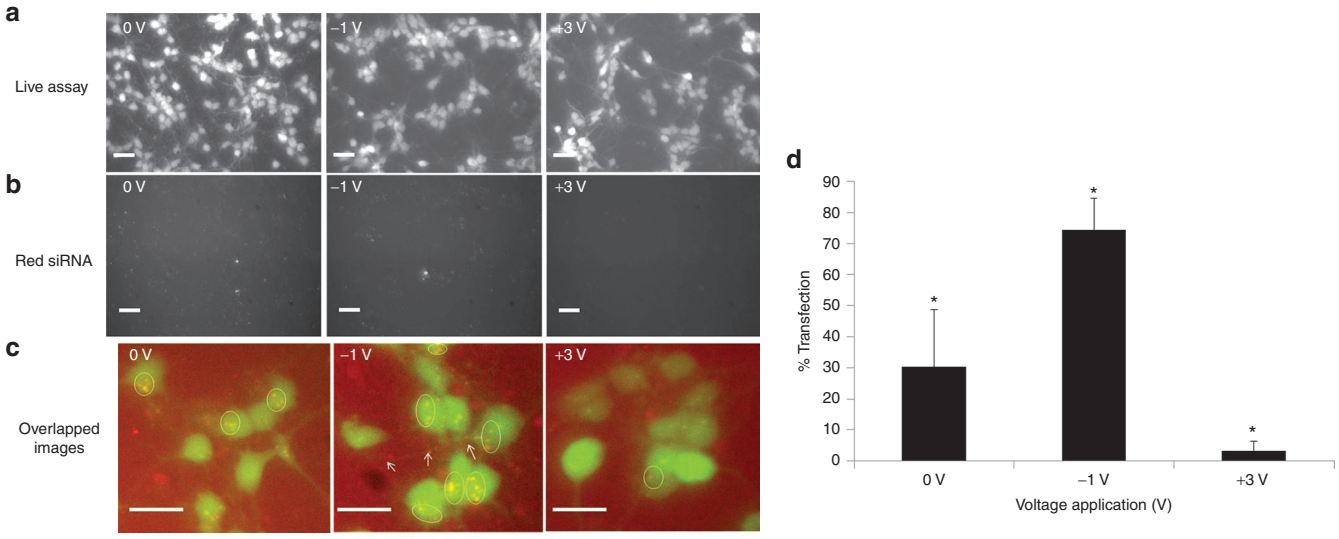

Figure 2 Voltage-controlled transfection of primary hippocampal neurons with Alexa-555 conjugated negative control siRNA (Invitrogen). (**a**) A standard live assay with calcein AM (Anaspec) was performed on siRNA transfected primary neurons (**b**) derived from E18 mice (Brainbits, LLC) preconditioned at different voltages at DIV 4 (days *in vitro*). (**c**) Closeup of primary neuronal cell bodies using overlapping live and red fluorescent images showed more transfection in −1 V preconditioned cells compared with 0 V or +3 V. Circled areas show transfected red dots within cells. In the −1 V image, evidence of transfection within neurites was indicated with arrows. (**d**) Transfection efficiencies were 30 ± 18% (n = 125 cells), 76 ± 10% (n = 59 cells), and 3 ± 3% (n = 67 cells) after preconditioning at 0, −1, and 3 V, respectively. Efficiencies were assessed over n = 4 overlapped images for calcein AM (live assay) and Alexa-555 conjugated siRNA for each preconditioning voltage using ImageJ software. Scale bar represents 50 µm. *Significance was assessed using Student's t-test corrected for multiple comparisons using Bonferroni criterion ($P < 0.003$).

In separate experiments, fluorescently tagged siRNA were loaded in PEI complexes, transfected into neuro2a cells at different pulse widths, and were subsequently imaged using DAPI nuclear stain (**Supplementary Figure S1**). Transfection efficiencies (computed using total cell counts obtained from DAPI) at 10 ms pulse width at different voltages were found to be comparable with those at corresponding voltages determined using the live assay in the earlier experiments (also with 10 ms pulse width; as shown in **Figure 3**). Transfection efficiencies were significantly lower (~29–33%) after preconditioning the cells with voltage pulses at +3 V and different pulse widths compared with 0 V (~61%). Conversely, after preconditioning at −1 V, the transfection efficiencies were marginally lower (76 ± 9.9%) at a pulse width of 1 ms compared with efficiencies of 90 ± 4.9% for a pulse width of 10 ms and 95 ± 4.5% for a pulse width of 100 ms. No significant changes in transfection efficiencies were observed after the application and removal of +3 V at different pulse widths (1–100 ms).

Modulated siRNA uptake within individual cells

In cells that were successfully transfected, there were variations in the level of siRNA uptake as indicated by pixel intensity distributions within individual cells (**Supplementary Figure S2**). The distribution of pixel intensities for 20 randomly picked cells for the case of PEI only transfection conditions (corresponding to 0 V controls) has lower median and interquartile distance than those after −0.5 V or −1 V preconditioning voltages. Similarly, cells preconditioned with ±2–3 V had lower median values and a narrower distribution of pixel intensities than those cells preconditioned between ±1 V. The presence

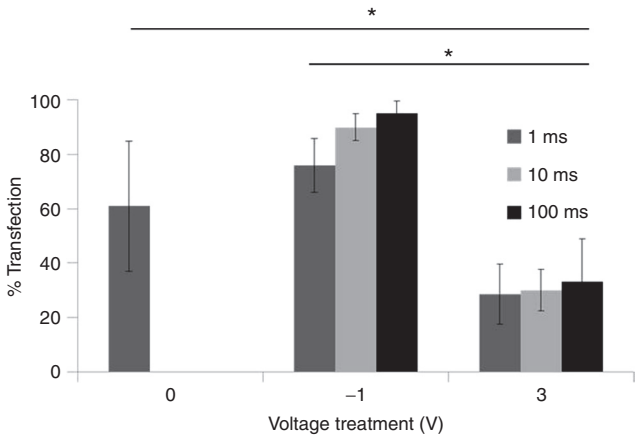

Figure 3 Comparison of transfection efficiencies of Alexa-555 conjugated control siRNA in neuro2a cells after different pulse widths (1, 10, and 100 ms) for the preconditioning voltage. Transfection efficiency was assessed using superimposed images of neuro2a cells using ImageJ with DAPI nuclear stain and transfected siRNA. Transfection efficiencies were calculated based on the ratio of cells with fluorescently tagged siRNA to total nuclei present in n = 4 images after 0 (no voltage), −1, and +3 V voltage preconditioning. Transfection efficiencies at 0 V were variable (61 ± 24%). At −1 V, transfection efficiencies were 76 ± 9.9% (1 ms pulse width), 90 ± 4.9% (10 ms pulse width), and 95 ± 4.5% (100 ms pulse width). At +3 V, transfection efficiencies were 29 ± 11% (1 ms pulse width), 30 ± 7.6% (10 ms pulse width), and 33 ± 16% (100 ms pulse width). *Significance was assessed using Student's t-test between 0 and −1 V and 0 and +3 V (post-hoc Bonferroni corrected $P < 0.006$). Two-way analysis of variance (ANOVA) used to assess significance between −1 and +3 V at all pulse widths ($P < 0.001$).

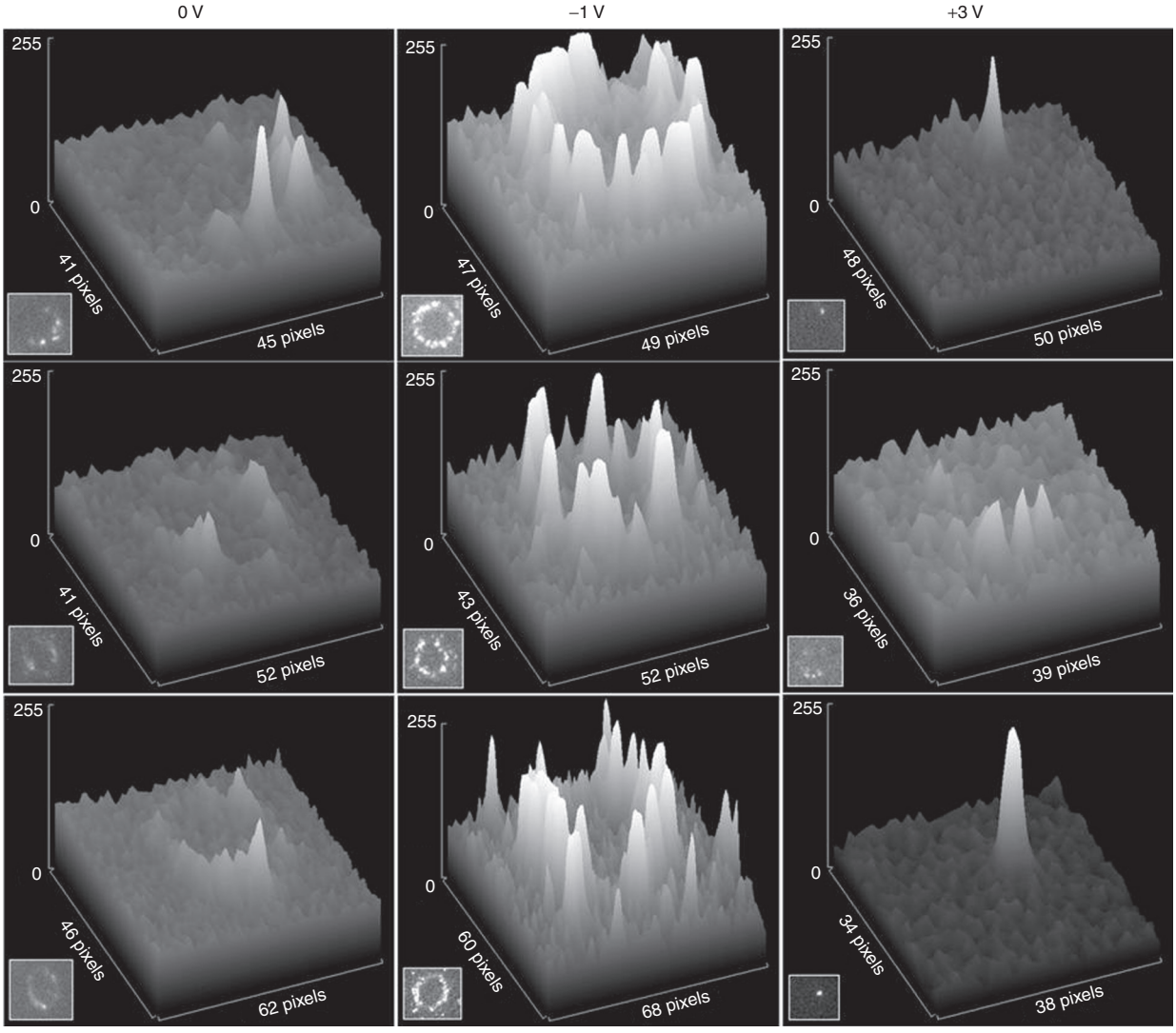

Figure 4 Representative single cell comparison of fluorescent intensity distributions of voltage-modulated transfection of Alexa-555 conjugated control siRNAin neuro2a cells at 10 ms pulse width. Individual cells (based on the nuclei-stained images in **Supplementary Figure S1**) were evaluated for the distribution of red pixels after preconditioning at 0 V (left), −1 V (middle), and +3 V (right) and transfection of Alexa-555 conjugated control siRNA. Pixel intensity information was derived from ImageJ and assessed for siRNA loading. Cells treated with −1 V had more loading overall compared with transfected cells in +3 V. Insets show representative cells with siRNA transfection.

of pixels with high intensities is indicative of higher density of siRNA in a given space within a cell. The intracellular, spatial distribution of siRNA in live cells was more uniform after preconditioning with −1 V compared with the spatial distribution in cells preconditioned at other voltages (**Figure 1**). Cells preconditioned with +3 V had distinguishable, intense spots of fluorescence inside the cell suggesting isolated, localized endocytosis of siRNA with much lower siRNA uptake compared with transfected cells after preconditioning with −1 V. The fluorescent siRNA intensity distribution of representative transfected cells from **Supplementary Figure S1** at each voltage level (10 ms pulse width) was individually analyzed as surface plots (**Figure 4**). As fluorescently tagged, negative control siRNA cannot enter the nucleus, the fluorescent intensity distribution was mainly located in the cytosol surrounding the nucleus. The relative change in pixel intensity from the center of the cell to the outer edge was ~132 ± 16 relative fluorescence units after preconditioning at −1 V, 73 ± 13 relative fluorescence units for 0 V, and negligible variation at +3 V. For the cells preconditioned with +3 V, non-uniform distribution of siRNA was observed with small highly intense, concentrated pixels that were 80–88 relative fluorescence units in the first two representative cells and 218 relative fluorescence units in the third cell in **Figure 4**. There was asymmetry in the distribution of siRNA around the nucleus. Fluorescent siRNA were found to coalesce closer in proximity to the nucleus regardless of the cell morphology (data not shown).

Figure 5a shows the variability in siRNA uptake (represented by the number of fluorescent pixels within each cell) in 20 different cells (raw data in **Figure 5b**) for each preconditioning voltage. The level of siRNA uptake within each cell was measured simply as the proportion of fluorescent pixels with intensities above background (determined using methods described in the image analysis section) to the total

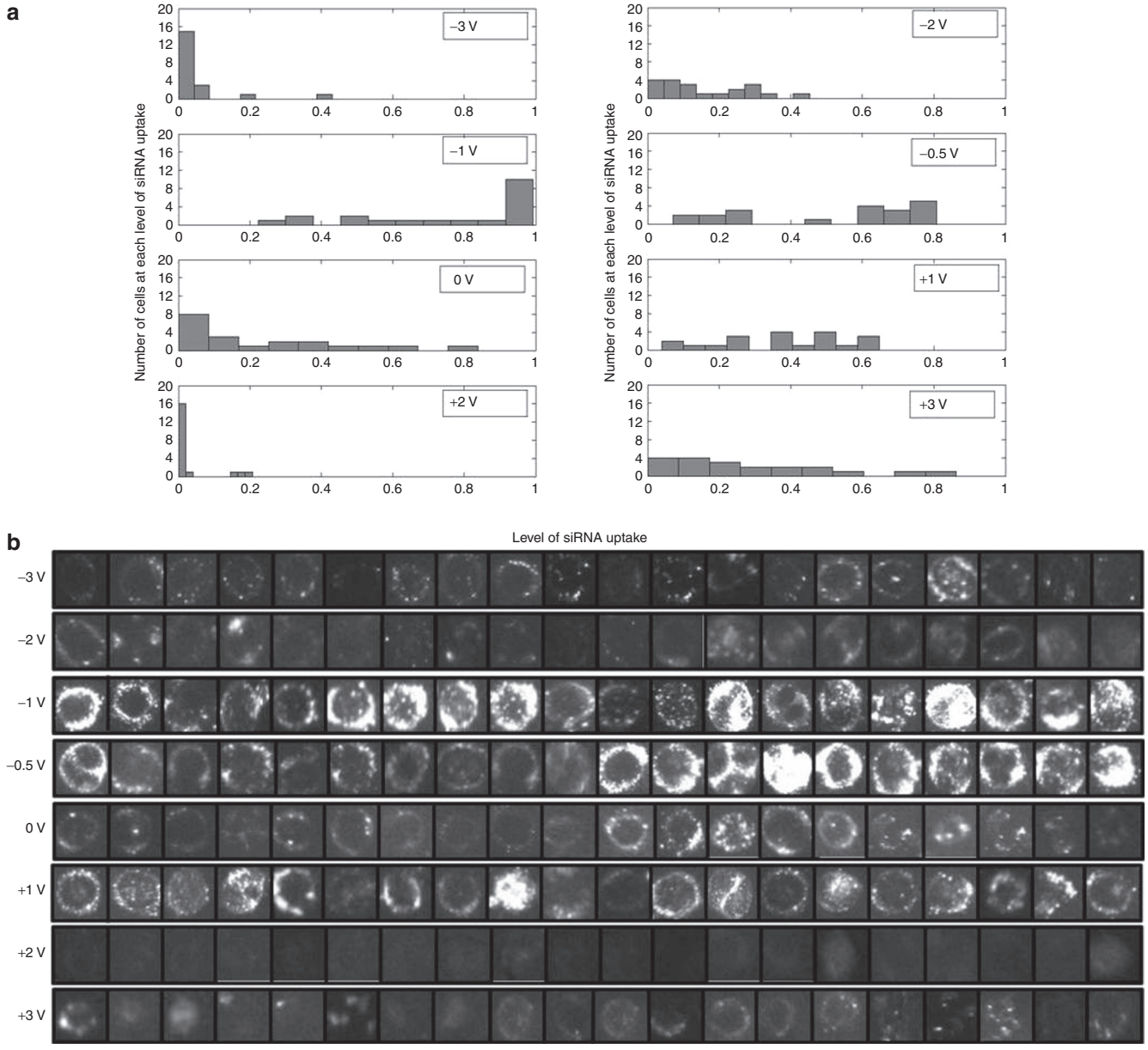

Figure 5 Modulated levels of siRNA uptake in neuro2a cells. (**a**) Using image analysis, the level of siRNA uptake in $n = 20$ cells for each preconditioning voltage was determined by the proportion of the number of red pixels (after background subtraction) for each cell normalized to the total number of pixels for an individual cell. The distribution of number of cells against the level of siRNA uptake (measured over a range of 0–1 and represented on the x-axis) was plotted for each preconditioning voltage (±3 V). siRNA uptake in cells with no preconditioning (0 V) were significantly lower compared with siRNA uptake at –1 V. siRNA uptake decreased from peak levels at –1 V to marginal levels at ±2–3 V. siRNA uptake after –1 to +1 V preconditioning was significantly different from those after +2 to 3 V ($P < 0.0001$). Significance was assessed using Student's *t*-test. (**b**) Cells ($n = 20$) from each preconditioning voltage were randomly selected and pooled for quantitative assessment of siRNA uptake.

number of pixels. Low fluorescent pixel count correspond to low siRNA uptake and high fluorescent pixel count correspond to high siRNA uptake. The level of siRNA uptake within a majority of the transfected cells was higher when preconditioned at –1 V than at 0 V (no preconditioning). Among the cells preconditioned at –1 V, some of the cells had approximately 90% siRNA uptake likely due to variations in cell cycle involving varying degrees of breakdown in the nuclear membrane, allowing for fluorescently tagged siRNA to distribute over a larger spatial area. In addition, the level of siRNA uptake within a majority of the transfected cells decreased as preconditioning voltages was increased from –1 V to +3 V. For preconditioning voltages of –2 V and –3 V, a dramatic decrease in siRNA uptake is observed. Large variations in siRNA uptake among individual cells is seen at 0 V (no preconditioning) with 40% of the measured cells showing only marginal siRNA uptake. Nevertheless, a trend of voltage-modulated siRNA uptake is observed despite moderate variations in siRNA uptake among preconditioned and transfected cells.

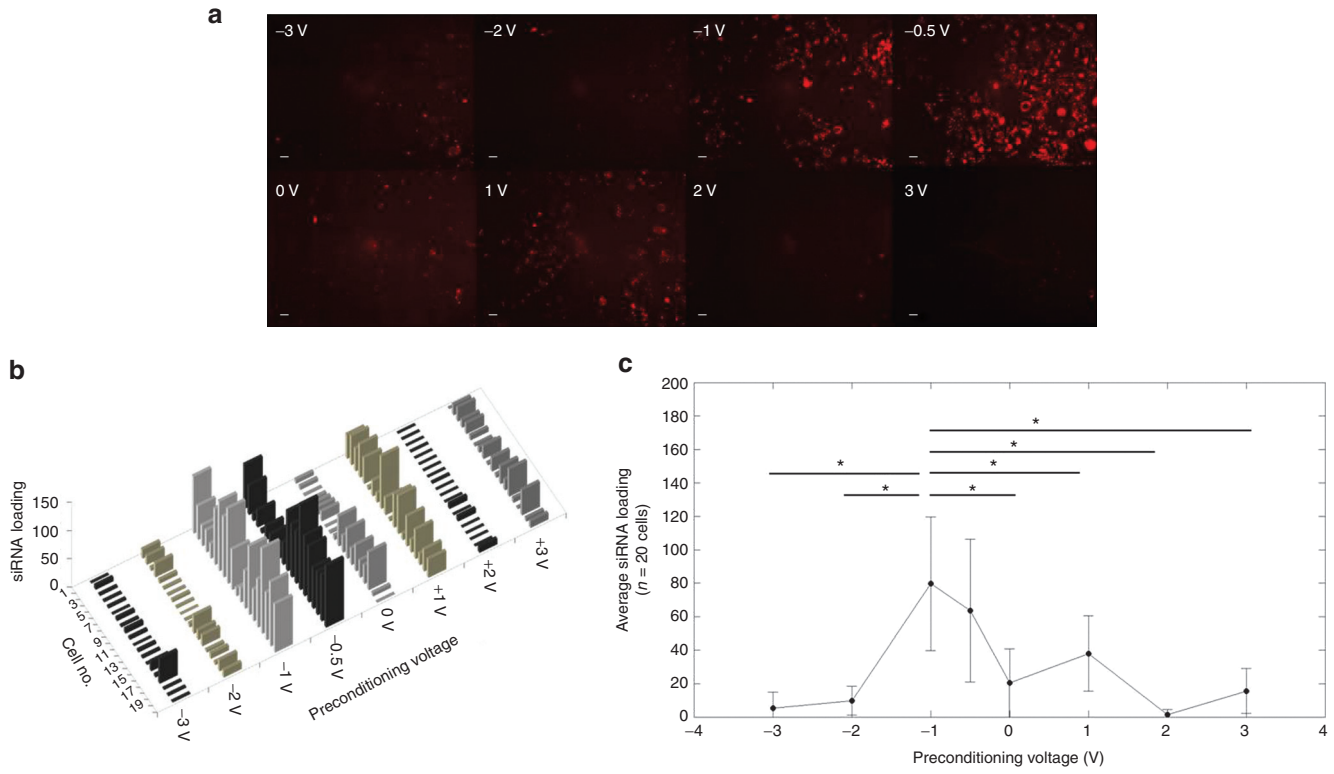

Figure 6 Quantification of siRNA loading after different preconditioning voltages in neuro2a cells. (**a**) Cells were preconditioned with different voltages at 10 ms pulse width and a sample of $n = 20$ cells pooled from multiple images were assessed for siRNA uptake (represented by the number of red fluorescent pixels within each cell) using MATLAB image processing toolbox. (**b**) Mean fluorescent signal intensity (calculated as the pixel intensity weighted by the fraction of pixels at each intensity above threshold) within each individual cell indicative of amount of siRNA loading is shown for each of the 20 cells after different preconditioning voltages. Preconditioning voltage-dependent siRNA loading is observed in individual cells. (**c**) A tuning curve of the average (±SD) of the mean pixel intensities in **b** (of $n = 20$ cells for each preconditioning voltage) for determining siRNA loading levels is shown for each preconditioning voltage. siRNA loading was highest after preconditioning at −1 V and lowest after preconditioning at ±2–3 V demonstrating an inverse relationship. *Statistically significant differences in the mean intensities were observed using Student's *t*-test between preconditioning at −1 V and preconditioning at (i) +1 V, (ii) ±2 V, and (iii) ± 3 V with $P < 0.0006$ (Bonferroni corrected for multiple comparisons), suggesting an optimal preconditioning voltage of −1 V for siRNA loading. Scale bar represents 100 µm.

Determination of the optimal preconditioning voltage and level of modulated siRNA loading in cells

To accurately quantify the level of siRNA loading (represented by both number of fluorescent pixels within each cell and their corresponding intensities), neuro2a cells were loaded with fluorescent siRNA using voltage preconditioning and imaged without additional contrast stains and analyzed for distribution of pixel intensities using MATLAB (**Figure 6a**). siRNA uptake and loading in cells were quantified for the voltage range of ± 3 V (eight different voltage levels). The mean intensity of pixels within each cell weighted by the fraction of pixels at each intensity level within each cell that is above background for 20 randomly chosen cells from each voltage application (total 160 cells) suggests a voltage-dependent siRNA loading in cells (**Figure 6b**). The distribution of pixel intensities (above background) in each of the transfected cells for each preconditioning voltage tested is shown in **Supplementary Figure S2a**. The aggregate distribution of pixel intensities (above background) of all 20 cells at each of the eight preconditioning voltages tested is shown in **Supplementary Figure S2b**. Finally, the distribution of pixel intensities in supplemental **Figure 2b** is used to calculate the mean intensity (plotted as mean ± SD of mean intensities of 20 cells) weighted by the number of pixels at each intensity (as a measure of siRNA loading in cells) and is plotted against the corresponding preconditioning voltage in **Figure 6c**. siRNA loading was ~3–4 times when cells are preconditioned with voltages between −1 V and 0 V compared with those preconditioned with 1 Vas shown in **Figure 6c**. It should be noted that even at voltages that inhibit transfection of PEI-siRNA complex (*i.e.,* have transfection efficiencies lower than that of PEI only without preconditioning) there is some low level of siRNA loading above background as observed in the range of 1–3 V in **Figure 6c**. Therefore, voltage preconditioning of cells modulated siRNA loading within transfected cells with less loading occurring at high voltages (+3 V) and maximal loading occurring at −1 V suggesting a controllable voltage-dependent siRNA loading phenomenon for small populations of cells.

Voltage-dependent functional silencing of GAPDH

Using GAPDH siRNA, we were able to show a voltage-dependent functional silencing in neuro2a cells using the voltage-preconditioning method (**Figure 7a**). Immunocytochemistry of cells using antibodies against GAPDH shows partial silencing

of GAPDH in cells 8 hours after transfection. A histogram analyzing the distribution of pixel intensities in representative individual cells after preconditioning at different voltages shows a large number of pixels at high intensity corresponding to endogenous levels of GAPDH and significantly smaller number of pixels at high intensities corresponding to preconditioning at 0 V and –1 V (**Figure 7b**). It is expected that as siRNA loading increases, the number of fluorescent pixels corresponding to GAPDH expression level will decrease due to siRNA induced inhibition. In a random sample of 20 cells from each preconditioning voltage, increased GAPDH siRNA loading levels in the individual cells caused significantly lower expressions of GAPDH (**Figure 7c**) after preconditioning at 0 V and –1 V ($P < 0.05$) using one-way analysis of variance (ANOVA). Significant reduction ($P < 0.006$ with post-hoc Bonferroni correction for multiple comparisons using Student's *t*-test) in GAPDH expression levels after preconditioning at –1 V and 0 V was also observed when compared with GAPDH expression levels after preconditioning at every other voltage (with and without GAPDH siRNA). Cells preconditioned with +3 V and transfected with GAPDH siRNA showed no significant difference in GAPDH levels compared with endogenous GAPDH levels in controls (one-way ANOVA, $P < 0.01$). Quantification of GAPDH expression in 20 randomly picked cells from $n = 3$ independent experiments shows an approximately twofold decrease in the mean level of GAPDH expression in cells preconditioned at –1 V to be compared with cells preconditioned at +3 V (**Figure 7c**). A highly correlative response between siRNA loading and functional silencing is also seen ($R^2 = 0.99$). Endogenous expression levels of GAPDH are not significantly different (one-way ANOVA, $P < 0.01$) in control experiments where cells were voltage preconditioned without GAPDH siRNA. For larger sample sizes (~150 cells per preconditioning voltage), GAPDH expression was significantly lower ($P < 0.01$ using one-way ANOVA) in cells preconditioned at –1 V compared with endogenous GAPDH levels corresponding to preconditioning voltages –1, 0, and 3 V. However, GAPDH expression in cells preconditioned at 0 V was not significantly different ($P < 0.01$ using one-way ANOVA) compared with endogenous GAPDH levels after preconditioning at –1, 0, and 3 V suggesting higher variability and lower level of knockdown in PEI only controls.

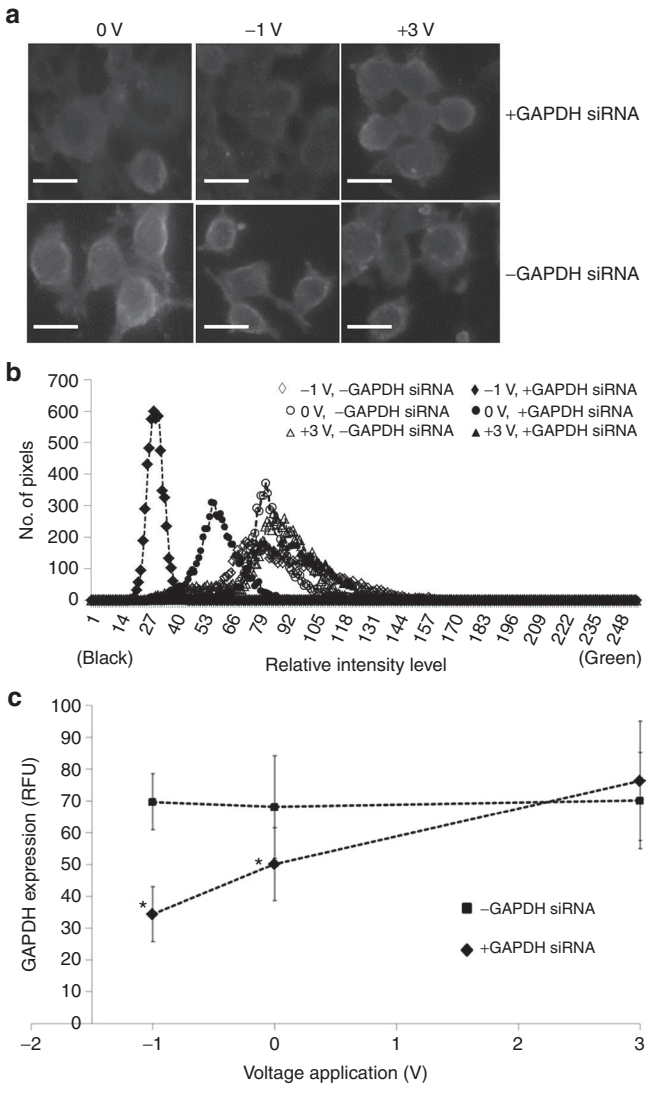

Figure 7 Analysis of GAPDH expression 8 hours after transfection in neuro2a cells treated with GAPDH siRNA. (**a**) Representative images of GAPDH expression in cells preconditioned at +3, 0, –1 V and treated with or without GAPDH siRNA. Cells were fixed and assessed for GAPDH expression using immunocytochemistry with fluorescently tagged antibodies. (**b**) Histograms of pixel intensities in representative individual cells after different preconditioning voltages. Filled points represent treatment with GAPDH siRNA after different preconditioning voltages, while unfilled points represent preconditioning at different voltages followed by no GAPDH siRNA. Diamonds (filled and open) correspond to –1 V preconditioning, circles (filled and open) correspond to 0 V preconditioning, and triangles (filled and open) correspond to +3 V preconditioning. Differential voltage-dependent siRNA loading in cells allows for modulated expression of GAPDH in cells. (**c**) Fluorescence was quantitatively determined as relative fluorescence units (RFUs) in $n = 20$ individual cells pooled from three independent experiments using ImageJ Squares represent samples not treated with GAPDH siRNA and diamonds represent samples treated with GAPDH siRNA. Statistical significance was assessed using one-way analysis of variance (ANOVA) with an α of 0.05. *Significance was further assessed for multiple comparisons between individual preconditioning voltages using a Student's *t*-test with Bonferroni correction, $P < 0.006$. Linear regression of GAPDH expression shows a high degree of correlation between the level of preconditioning voltage and level of GAPDH expression. The mean GAPDH expression level in cells preconditioned with +3 V is over twice as high as the mean GAPDH expression level in cells preconditioned with –1 V.

Voltage-dependent functional silencing in primary hippocampal neurons

Using siRNA directed against BDNF, we showed the effects of modulated functional silencing on dendrite morphology visualized using antibodies for microtubule associated protein-2 (MAP-2) (**Figure 8**). Primary hippocampal neurons (DIV4) were treated with BDNF siRNA after preconditioning at –1 V (for high siRNA loading), +3 V (for low siRNA loading), and 0 V (PEI only–moderate siRNA loading). Live assays showed similar cell densities and level of neurite extensions 8 hours after transfection (**Figure 8a–e**). Major changes in morphology of neuronal dendrites and neuronal cell densities were visualized using MAP-2 antibodies 24 hours after transfection (**Figure 8f–j**). A decreased cell

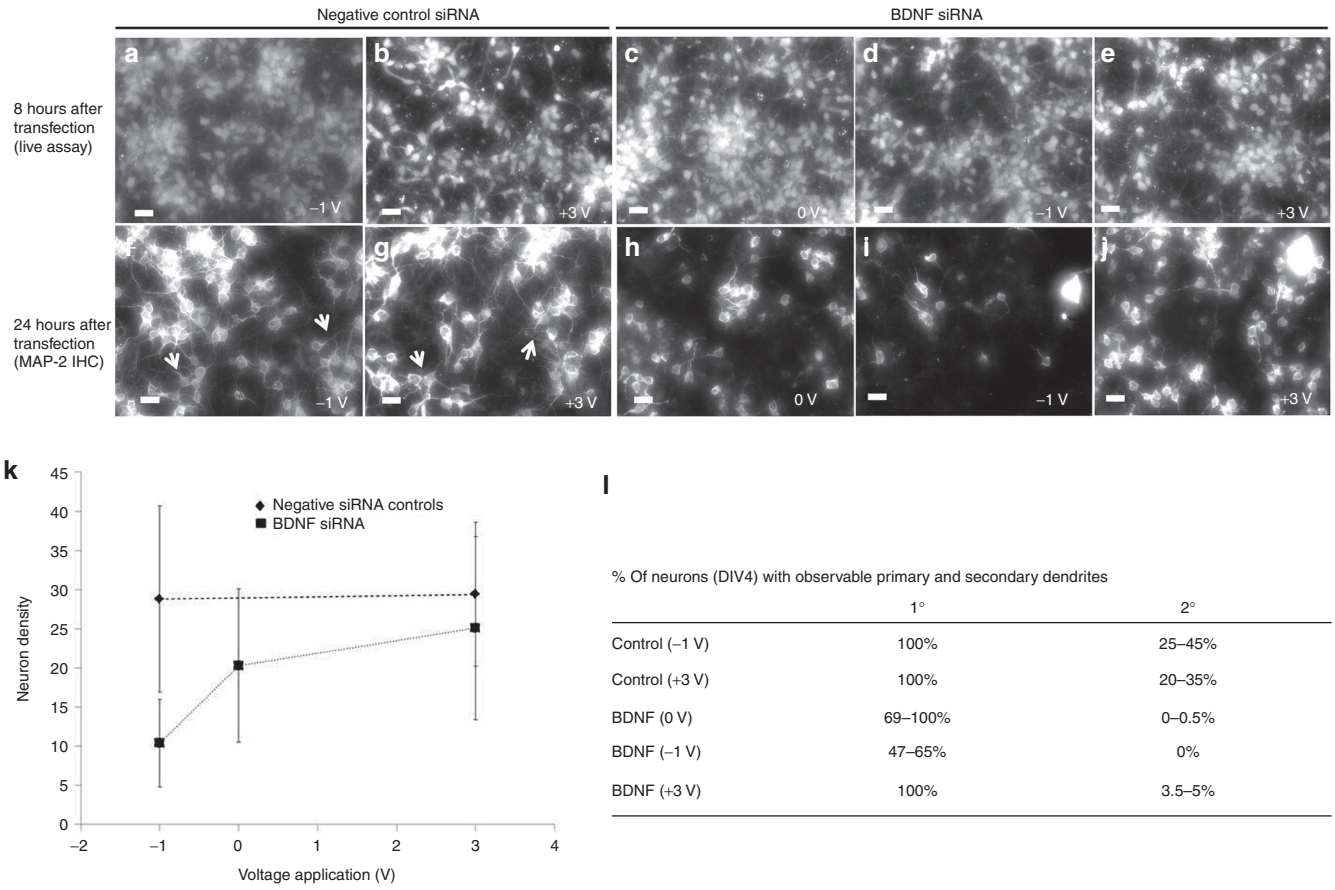

Figure 8 Modulated silencing of brain derived neurotrophic factor (BDNF) in primary hippocampal neurons (DIV4). (**a**–**e**) Live assays of primary neuron cultures were taken 8 hours after BDNF siRNA transfection using the voltage-preconditioning method. After 8 hours, cell densities and morphologies were similar between cells (**a**,**b**) transfected with negative controls and those (**c**–**e**) transfected with BDNF siRNA. (**f**–**j**) Twenty-four hours after transfection, cells were fixed and evaluated for morphology using immunohistochemistry with MAP-2 antibodies. (**f**,**g**) Neurite/dendrite morphology in controls showed high degree of secondary and tertiary branching (arrows) and relatively similar cell densities. BDNF siRNA transfected cells showed decreased cell densities after preconditioning at –1 V (corresponding to high siRNA loading) compared with those of cells preconditioned at 0 and +3 V. (**h**) Cells preconditioned at +3 V (corresponding to low siRNA loading) and treated with BDNF siRNA showed similar cell densities as controls but exhibited loss of neurite branching and complexity compared with controls. Scale bars represent 50 µm. (**k**) Neuron density and percentage of neurons with (**l**) observable primary and secondary dendrites was quantified using ImageJ with MAP-2–stained images ($n = 5$).

density is observed in cells preconditioned with –1 V compared with cells preconditioned with 0 V, +3 V, and those with negative controls (**Figure 8k**). Neurons preconditioned at +3 V and treated with BDNF siRNA (**Figure 8j**) were similar in cell density compared with negative controls (**Figure 8f,g**). Among neurons in the negative controls (**Figure 8f,g**), two to five primary neurites emanated from the main cell body compared with typically one neurite extending out from BDNF siRNA loaded cells in (**Figure 8h–j**). Secondary and tertiary branching in neurites were prominent in controls (indicated by arrows) and nonexistent in BDNF siRNA loaded neurons preconditioned cells at +3, 0, and –1 V.

Discussion

Controlling delivery and dosage of genetic constructs in cells can be labor-intensive and low-yielding process requiring accurate positioning of cells within devices typically by microinjection or nanoelectroporation of a small membrane patch.[31] Alternative high-throughput methodologies that use spotting techniques or microfluidic delivery of genetic constructs have shown controlled uptake of DNA and genetic constructs but they still have to rely on the inherent, natural endocytotic ability of the cell to take up the gene construct.[37,39,40] This may lead to variability in gene expression among individual cells as observed in our current study in the case PEI-siRNA control transfections with no preconditioning. In this study, we demonstrate a unique voltage preconditioning approach in combination with a conventional chemical transfection technique that can be readily modified and possibly complement current high-throughput technologies for difficult-to-transfect adherent neuro2a cells and primary neurons.

The proposed hybrid technique is rapid, consistent, repeatable and scalable to high-throughput applications and takes <10 minutes for the entire protocol which can be further reduced with automation. The cell viability is virtually unaffected by the reported technique. In addition, analysis of the GAPDH expression levels in voltage-preconditioned cells

in control experiments suggests endogenous levels are not affected by voltage preconditioning. In comparison with typical PEI-based transfection of siRNA, voltage-controlled PEI/siRNA complex delivery showed (i) less variability and (ii) rapid assimilation of siRNA in cells with (iii) higher efficiency. Control experiments involving transfection with PEI only without preconditioning yielded high variability in transfection efficiency (± 24%). PEI-based transfection of siRNA in literature is known for notoriously low levels of transfection in difficult-to transfect cells like primary neurons as demonstrated in our current study without any preconditioning voltage. For primary neurons, the observed transfection efficiency using only PEI and no preconditioning was significantly lower than the corresponding values for neuro2a cells possibly due to the level of differentiation and relative cell size. High levels of siRNA loading could be achieved using the voltage-preconditioning method for both neuro2a and primary hippocampal neurons in culture, suggesting a broader application of the technique across multiple neuron-like cell types. Approximately, four-times increase in cell loading of siRNA was demonstrated using preconditioning at –1 and –0.5 V compared with siRNA loading under no preconditioning (0 V) or 2 V preconditioning (**Figure 6c**). In addition, and interestingly, almost complete inhibition of PEI mediated transfection was demonstrated for voltages outside the –1 to 1 V window.

The voltage-modulated uptake and loading of siRNA is likely due to a combination of mechanisms. Enhanced endocytosis of the siRNA is hypothesized to be one of the mechanisms because preconditioned cells have highly intense points of fluorescence within cells suggesting a localized concentration effect typical of the endosomal pathway. In a large fraction of the cells, an asymmetric distribution of fluorescent siRNA is observed closely packed around the nucleus, with one side of the nucleus having a larger amount of siRNA than the others. This observation is similar to microtubule associated endocytosis, which is one of the prominent mechanisms of PEI-based transfection.[41] Also, attempts to precondition cells at –1 V using cold buffer (4 °C) (which is expected to shut down endocytosis) showed negligible or low siRNA uptake, suggesting endocytosis is an essential mechanism for voltage preconditioning facilitated siRNA uptake (data not shown). At higher voltages, preconditioned cells have a lower uptake of siRNA, suggesting that the natural endocytotic pathways may be less conducive to internalization at higher electric field intensities. Enhanced uptake has been observed in cells using the electro-endocytosis mechanism in other mammalian cells.[42,43] Although electro-endocytosis has been shown to enhance uptake using long, low voltage pulse trains (upto 10 minutes) that are applied during transfection, here, we show controllable, enhanced uptake with the application of three different voltage pulses (each within ±3 V) over a duration of <10 ms per pulse before the administration of PEI-siRNA complex. For pulse durations of 100 ms and for pulse numbers >10, partial delamination of cells from the indium tin oxide (ITO) surface was observed in some samples.

Electrochemical characterization of ITO surface with voltage-preconditioned neuro2a cells indicated no significant change in the impedance spectra of the ITO surface due to preconditioning. This indicates no significant change in the cell coverage of the ITO surface and the charge transfer properties at the interface. Previous studies have shown transient changes in cell surface charges due to the application of electric fields.[44,45] In our study, cyclic voltammagrams of electrodes with cells showed that the electrode-cell surface interface had higher charge storage capacitance compared with electrodes without any cells (results not shown here). The typical range of voltages over which the cyclic voltammograms were capacitive was –1.4 to 0.7 V. Beyond this range, redox current peaks corresponding to hydrolysis and other faradaic reactions were observed.

A possible explanation for the inhibition of siRNA loading at higher voltages could be due to a cell surface charge redistribution effect that may repel the PEI-siRNA complex in conjunction with changes in the protein conformations that may inhibit the endocytosis pathway. In addition, the modulation of siRNA loading using (i) different voltages and (ii) different pulse widths at –1 V suggests that the electroaffinity of the PEI/siRNA complex to the cell surface may also play a role. The increase in transfection efficiency of neuro2a cells and primary neurons preconditioned with slightly negative voltages could be due to the enhanced electrostatic attraction with PEI/siRNA that are known to form nanoparticle complexes with typical zeta potentials (~50–70 mV).[18] There was no uptake of naked siRNA in cells after similar voltage treatments. The voltage-dependent cell loading therefore could be a combination of electrostatic attraction of siRNA complexes due to the charge redistribution of a transiently high capacitive cell layer and an enhanced endocytotic response.

Electroporation and membrane breakdown is not expected as a mechanism of siRNA transfer due to low electric field strengths (<30 V/cm). For electroporative gene transfer, a minimum of 0.3 kV/cm was found to be necessary for transfection.[24] COMSOL simulations (results not shown) indicate that electric field intensities are at least one to two orders below the range typically required for electroporation. In addition, experiments involving voltage-preconditioned cells with propidium iodide dye, a classic marker to study diffusion due to electroporative pore formation, show no cellular uptake at –1 V (**Supplementary Figure S3**). Further experiments are needed to better understand the synergistic contributions of electrokinetic attraction and the electroendocytotic pathway. Nevertheless, it is clear that a manipulation of the cell surface using voltage preconditioning is necessary for modulating the delivery of PEI-siRNA complexes.

GAPDH typically has high expression in a cell and is relevant in the energy metabolism in neurons and neuron-like cells, and therefore commonly used as a housekeeping gene control in experiments. We saw proportional, partial knockdown in GAPDH expression for a given stock concentration of siRNA 8 hours after transfection, which is consistent with previous reports in literature.[16] Up to twofold changes in GAPDH expression levels were demonstrated due to silencing. The level of gene silencing is, however, expected to be dependent on the level of corresponding endogenous gene expression in individual cells at any given time. The functional effect is likely to be more dramatic in genes that have lower expression levels. The preconditioning protocol presented here needs to optimized for individual genes and cell type. Changes in primary hippocampal neuronal morphology were effectively demonstrated with modulated BDNF knockdown

using voltage preconditioning. Modulated BDNF expression levels have been implicated in various neurodegenerative disease states including Alzheimer's disease.[46] At low levels of BDNF siRNA loading (+3 V), cell densities were maintained, but significant changes in dendritic branching were seen in comparison with negative controls (**Figure 8l**). Alternate means of optimizing and controlling siRNA loading can be achieved by varying exposure time, point of application, and variation in voltage pulse numbers. Modulation of gene expression in neurodegenerative diseases plays a key role in the manifestation and severity of disease symptoms. For instance, different levels of expression of (α)-synucleingene has been shown to determine the degree of severity in Parkinson's disease.[47] Partial gene knockout studies in Alzheimer's disease show alleviation of symptoms, revealing that a potential strategy for gene therapy is a dose-dependent reduction of a putative gene.[22,48] Expression levels of APOE-4 gene are also correlated to disease manifestation in nonfamilial Alzheimer's disease.[49,50] From a biological perspective, dose-dependent gene expression plays a significant role in neurodegenerative diseases. So, it can be argued that smart, controlled delivery of therapeutics will also be critical[51] for drug efficacy. Therefore, there is a need to develop a strategy for controlled delivery of genetic constructs to neurons and neuron-like cells and then assess the therapeutic effects of modulated gene silencing. The main objective of this paper is to demonstrate a novel voltage-preconditioning strategy to achieve controlled, modulated delivery of siRNA in an *in vitro* culture to functionally silence relevant genes.

In conclusion, the voltage-modulated siRNA cell loading method could be incorporated into medium and high-throughput systems for high-yielding, uniform transfection. This study successfully combines the major advantages of electric field–assisted gene delivery such as rapid delivery and tenability with conventional chemical transfection techniques.

Materials and methods

Preparation of cell culture in indium tin oxide wells. ITO substrates were purchased from Delta Technologies (Madison, WI) with resistances 10–12/sq resistance. Glass wells (1 cm diameter) were attached to the substrates with polydimethylsiloxane (Sylgard 184; Dow Corning, Midland, MI) polymer. Before cell seeding, the ITO-based cell culture wells were thoroughly cleaned, and incubated with 1 mol/l sodium hydroxide for 15 minutes to remove organic residues. Next, the wells were thoroughly washed with distilled water six times, dried, and autoclaved for sterility. Neuro2a cells were seeded at ~3,000 cells and grown at 37 °C for 24 hours before transfection in 10% fetal bovine serum, 1% antibiotics, advanced MEM media (catalog#12492-Gibco, Life Technologies, Grand Island, NY). Primary hippocampal neurons (E18 mice) were purchased from (Brainbits, Llc, Springfield, IL) and seeded at 3,000–5,000 cells per well. The cells were allowed to grow and differentiate till DIV4 before transfection.

Voltage-controlled siRNA transfection. For siRNA transfection, AF 555 conjugated negative control siRNA (Qiagen, Valencia, CA) with target sequence (5′-CAGGGTATCGACGATTACAAA-3′(AF555)) and GAPDH siRNA (Qiagen) with sequence (5′-CCGAGCCACATCGCTCAGACA-3′) was used. BDNF siRNA (#sc-42122; Santa Cruz Biotechnologies, Santa Cruz, CA) was used in functional silencing of primary hippocampal neurons. Branched polyethylenimine of 25 K was bought from Sigma Aldrich (CAS#9002-98-6; St Louis, MO). PEI/siRNA nanocomplexes with N/P ratios of 30 were mixed in deionized water and incubated for 20–30 minutes at room temperature. Typically, 0.5–1 pmol of siRNA was used for a reaction. Cells were prepared by washing two times with phosphate-buffered saline (PBS) and filled with 300 µl of PBS without calcium or magnesium. Using a voltage pulse generator (Pragmatic 2414A waveform generator; Tegam, Geneva, OH), cells were exposed to square wave pulse trains (n = 1–10) with a 50% duty cycle in the range of ±3 V. Pulse widths were varied between 1, 10, and 100 ms. Optimal pulse trains used bursts of n = 3 cycles. Immediately after exposure to various voltages, the cells were incubated with preformed complexes of PEI/siRNA for 10 minutes. After the exposure, PBS was aspirated and replaced with media. Live assays were performed by 20 minutes incubation with calcein AM (Anaspec, Fremont, CA). DAPI (Invitrogen, Carlsbad, CA) was used for imaging cell nuclei in some experiments. Image acquisition was done 4–8 hours after transfection using appropriate filters and a Leica DFC345Fx monochromatic camera (Leica Microsystems, Wetzlar, Germany) with advanced fluorescence suite.

Immunocytochemistry. Fluorescent scrambled siRNA, GAPDH siRNA, and BDNF siRNA treated neurons were prepared for immunocytochemistry 18–24 hours preconditioning. Briefly, cells were fixed washed once in 1X PBS and fixed in 4% paraformaldehyde for 15 minutes. After permeation with 0.1% Triton X (10 minutes), the fixed cells were incubated in 1% bovine serum albumin for 30 minutes. The cells were rinsed in PBS and incubated with either mouse monoclonal GAPDH antibody (AbCam, Cambridge, UK) diluted 1:500 in PBS or mouse monoclonal MAP-2 antibody (Sigma) diluted 1:500 in PBS for 2 hours. After the cells were rinsed in PBS (3X), the cells were incubated with fluorescently tagged (Alexa-488) secondary antibodies (Invitrogen) diluted 1:1000 in PBS for 1 hour. Cells were again washed in PBS (2X) and visualized using fluorescence microscopy.

Image analysis. For live assay, percentage transfection was calculated in n = 4 images and calculated as the ratio of number of cells with siRNA fluorescence (ex555) regardless of specific loading intensity and the number of calcein AM (ex488)–stained cells. For DAPI-based assays, images were acquired using two different filters and superimposed using ImageJ (National Institutes of Health, Bethesda, MD). Transfection efficiencies were calculated in n = 4 images as the ratio of number of cells with siRNA fluorescence surrounding a nucleus divided by the number of DAPI-stained nuclei. Each DAPI-stained nucleus was counted as one cell. For live and DAPI-based assays, the cells were counted and analyzed using ImageJ (National Institutes of Health). Statistical significance between preconditioning voltages was assessed using Student's t-test with $P < 0.001$.

Image acquisition used the same acquisition time and settings to accurately capture the fluorescence intensity changes due to modulated siRNA loading within cells.

The raw acquired images were imported to MATLAB and analyzed using the image processing toolbox. For whole image analysis, the distribution of pixel intensities was determined using boxplots and compared with background samples. Ten background samples representing areas (approximately 150 × 150 pixels) in the image with no cells were collected for each image and preconditioning voltage. A boxplot of pixel intensity distributions corresponding to the background was determined. The intensity level on background samples corresponding to the upper whisker on the boxplot (representing 1.5 times the difference between the 25% percentile marker and the 75% percentile marker) was taken as the threshold for positive signal. Therefore, the threshold was defined as:

$$T = Q_3 + 1.5\,(Q_3 - Q_1) \quad (1)$$

where T is threshold value, Q_1 is the 25% percentile marker for all data points, and Q_3 is the 75% percentile marker for all data points. Outliers were defined as pixels with intensities exceeding the threshold "T." In a boxplot of normally distributed pixel intensities, for instance, 99.8% of pixels will have intensities lower than the threshold intensity. Similar threshold markers were used for single cell analyses. Pixels in a cell with intensities above the threshold were considered as positive signal and pixels below the threshold considered as background. To assess the siRNA uptake quantitatively, boxplots of signal distribution after background subtraction were used to calculate the number of pixels above background. To assess the level of siRNA uptake (**Figure 5**), the proportion of signal pixels that exceed threshold to total number of pixels in individual cells were assessed for $n = 20$ cells for every preconditioning voltage. To assess siRNA loading, mean intensity was determined by weighting each intensity exceeding threshold by the number of pixels at that intensity (**Figure 6b,c**), normalized to the total number of pixels in each cell image. Significant differences (Bonferroni corrected for multiple comparisons, $P < 0.0006$) were found using Student's *t*-test between siRNA loading after preconditioning at −1 V compared with siRNA loading after preconditioning at any one of the following voltages −3, −2, 0, +1, +2, and +3 V.

For immunocytochemistry studies with GAPDH siRNA, quantitative values for pixel-based fluorescent intensity values were generated using ImageJ. Typical distribution of pixel intensities in a cell for each preconditioning voltage is plotted in **Figure 7b**. For **Figure 7c**, the histograms of pixel intensities (ranging 0–255) for $n = 20$ individual cells from three independent experiments for each preconditioning voltage (−1, 0, and 3 V) was generated using ImageJ. The intensity value with the highest number of pixels was determined for each cell ($n = 20$) as representative of its GAPDH expression. Statistical significance was assessed using one-way ANOVA (α of 0.05). Significance was further assessed for multiple comparisons between individual preconditioning voltages using a Student's *t*-test with a Bonferroni correction at $P < 0.006$. For all larger image samples, background subtraction for each image of cells with threshold criteria as in equation 1 was used. A pixel with GAPDH signal was a pixel with intensity value above the threshold criteria. A product of the median intensity of the fluorescent pixels (that are above threshold or background) within every cell in the image and the number of fluorescent pixels within that cell was calculated. The product was subsequently normalized to cell count in $n = 3$ independent experiments. Statistical significance in GAPDH expression levels was first assessed using one-way ANOVA at $P < 0.01$. GAPDH expression levels after preconditioning at −1 V and GAPDH siRNA treatment was compared with endogenous GAPDH levels after preconditioning at all voltages. Similar comparison for GAPDH expression levels after preconditioning at 0 V and GAPDH siRNA treatment. Subsequently, Student's *t*-test ($P < 0.01$) was used to compare GAPDH expression levels after preconditioning at −1 V with GAPDH expression levels at every other preconditioning voltage. Similar pair-wise *t*-tests were also performed for GAPDH expression levels after preconditioning at 0 V.

Supplementary material

Figure S1. Representative images of voltage modulated transfection of Alexa-555 conjugated negative control siRNA (Invitrogen) under different pulse width conditions.
Figure S2. Intensity distribution in individual cells ($n = 20$) for each voltage application.
Figure S3. Propidium iodide uptake in voltage-preconditioned cells.

Acknowledgments. This work was supported by Alzheimer's Core Disease Center (ADCC) proposal #10087351 and the National Institutes of Health Ruth L Kirschstein fellowship (5F32NS073422-02) for AS. The authors declared no conflict of interest.

1. Urban-Klein, B, Werth, S, Abuharbeid, S, Czubayko, F and Aigner, A (2005). RNAi-mediated gene-targeting through systemic application of polyethylenimine (PEI)-complexed siRNA in vivo. *Gene Ther* **12**: 461–466.
2. Horbinski, C, Stachowiak, MK, Higgins, D and Finnegan, SG (2001). Polyethyleneimine-mediated transfection of cultured postmitotic neurons from rat sympathetic ganglia and adult human retina. *BMC Neurosci* **2**: 2.
3. Ohki, EC, Tilkins, ML, Ciccarone, VC and Price, PJ (2001). Improving the transfection efficiency of post-mitotic neurons. *J Neurosci Methods* **112**: 95–99.
4. Dalby, B, Cates, S, Harris, A, Ohki, EC, Tilkins, ML, Price, PJ et al. (2004). Advanced transfection with Lipofectamine 2000 reagent: primary neurons, siRNA, and high-throughput applications. *Methods* **33**: 95–103.
5. Zhang, C, Yadava, P and Hughes, J (2004). Polyethylenimine strategies for plasmid delivery to brain-derived cells. *Methods* **33**: 144–150.
6. Lee, WG, Demirci, U and Khademhosseini, A (2009). Microscale electroporation: challenges and perspectives for clinical applications. *Integr Biol (Camb)* **1**: 242–251.
7. Boussif, O, Lezoualc'h, F, Zanta, MA, Mergny, MD, Scherman, D, Demeneix, B et al. (1995). A versatile vector for gene and oligonucleotide transfer into cells in culture and in vivo: polyethylenimine. *Proc Natl Acad Sci USA* **92**: 7297–7301.
8. Kwok, A and Hart, SL (2011). Comparative structural and functional studies of nanoparticle formulations for DNA and siRNA delivery. *Nanomedicine* **7**: 210–219.
9. Shim, MS and Kwon, YJ (2009). Acid-responsive linear polyethylenimine for efficient, specific, and biocompatible siRNA delivery. *Bioconjug Chem* **20**: 488–499.
10. Zintchenko, A, Philipp, A, Dehshahri, A and Wagner, E (2008). Simple modifications of branched PEI lead to highly efficient siRNA carriers with low toxicity. *Bioconjug Chem* **19**: 1448–1455.
11. Höbel, S and Aigner, A (2010). Polyethylenimine (PEI)/siRNA-mediated gene knockdown in vitro and in vivo. *Methods Mol Biol* **623**: 283–297.
12. Ulasov, AV, Khramtsov, YV, Trusov, GA, Rosenkranz, AA, Sverdlov, ED and Sobolev, AS (2011). Properties of PEI-based polyplex nanoparticles that correlate with their transfection efficacy. *Mol Ther* **19**: 103–112.
13. Wong, Y, Markham, K, Xu, ZP, Chen, M, Max Lu, GQ, Bartlett, PF et al. (2010). Efficient delivery of siRNA to cortical neurons using layered double hydroxide nanoparticles. *Biomaterials* **31**: 8770–8779.
14. Wong, Y, Cooper, HM, Zhang, K, Chen, M, Bartlett, P and Xu, ZP (2012). Efficiency of layered double hydroxide nanoparticle-mediated delivery of siRNA is determined by nucleotide sequence. *J Colloid Interface Sci* **369**: 453–459.
15. White, AK, VanInsberghe, M, Petriv, OI, Hamidi, M, Sikorski, D, Marra, MA et al. (2011). High-throughput microfluidic single-cell RT-qPCR. *Proc Natl Acad Sci USA* **108**: 13999–14004.

16. Toriello, NM, Douglas, ES, Thaitrong, N, Hsiao, SC, Francis, MB, Bertozzi, CR et al. (2008). Integrated microfluidic bioprocessor for single-cell gene expression analysis. *Proc Natl Acad Sci USA* **105**: 20173–20178.
17. Wang, D and Bodovitz, S (2010). Single cell analysis: the new frontier in 'omics'. *Trends Biotechnol* **28**: 281–290.
18. Grayson, AC, Doody, AM and Putnam, D (2006). Biophysical and structural characterization of polyethylenimine-mediated siRNA delivery in vitro. *Pharm Res* **23**: 1868–1876.
19. Hufnagel, H, Hakim, P, Lima, A and Hollfelder, F (2009). Fluid phase endocytosis contributes to transfection of DNA by PEI-25. *Mol Ther* **17**: 1411–1417.
20. Dominska, M and Dykxhoorn, DM (2010). Breaking down the barriers: siRNA delivery and endosome escape. *J Cell Sci* **123**(Pt 8): 1183–1189.
21. Akinc, A, Thomas, M, Klibanov, AM and Langer, R (2005). Exploring polyethylenimine-mediated DNA transfection and the proton sponge hypothesis. *J Gene Med* **7**: 657–663.
22. Laird, FM, Cai, H, Savonenko, AV, Farah, MH, He, K, Melnikova, T et al. (2005). BACE1, a major determinant of selective vulnerability of the brain to amyloid-beta amyloidogenesis, is essential for cognitive, emotional, and synaptic functions. *J Neurosci* **25**: 11693–11709.
23. Karra, D and Dahm, R (2010). Transfection techniques for neuronal cells. *J Neurosci* **30**: 6171–6177.
24. Kanduser, M, Miklavcic, D and Pavlin, M (2009). Mechanisms involved in gene electrotransfer using high- and low-voltage pulses–an in vitro study. *Bioelectrochemistry* **74**: 265–271.
25. Jordan, ET, Collins, M, Terefe, J, Ugozzoli, L and Rubio, T (2008). Optimizing electroporation conditions in primary and other difficult-to-transfect cells. *J Biomol Tech* **19**: 328–334.
26. Stroh, T, Erben, U, Kühl, AA, Zeitz, M and Siegmund, B (2010). Combined pulse electroporation–a novel strategy for highly efficient transfection of human and mouse cells. *PLoS ONE* **5**: e9488.
27. Jain, T and Muthuswamy, J (2007). Bio-chip for spatially controlled transfection of nucleic acid payloads into cells in a culture. *Lab Chip* **7**: 1004–1011.
28. Jain, T and Muthuswamy, J (2008). Microelectrode array (MEA) platform for targeted neuronal transfection and recording. *IEEE Trans Biomed Eng* **55**(2 Pt 2): 827–832.
29. Jain, T and Muthuswamy, J (2007). Microsystem for transfection of exogenous molecules with spatio-temporal control into adherent cells. *Biosens Bioelectron* **22**: 863–870.
30. Selmeczi, D, Hansen, TS, Met, O, Svane, IM and Larsen, NB (2011). Efficient large volume electroporation of dendritic cells through micrometer scale manipulation of flow in a disposable polymer chip. *Biomed Microdevices* **13**: 383–392.
31. Boukany, PE, Morss, A, Liao, WC, Henslee, B, Jung, H, Zhang, X et al. (2011). Nanochannel electroporation delivers precise amounts of biomolecules into living cells. *Nat Nanotechnol* **6**: 747–754.
32. Weecharangsan, W, Opanasopit, P and Lee, RJ (2007). In vitro gene transfer using cationic vectors, electroporation and their combination. *Anticancer Res* **27**(1A): 309–313.
33. Coulberson, AL, Hud, NV, LeDoux, JM, Vilfan, ID and Prausnitz, MR (2003). Gene packaging with lipids, peptides and viruses inhibits transfection by electroporation in vitro. *J Control Release* **86**: 361–370.
34. Wang, S, Zhang, X, Yu, B, Lee, RJ and Lee, LJ (2010). Targeted nanoparticles enhanced flow electroporation of antisense oligonucleotides in leukemia cells. *Biosens Bioelectron* **26**: 778–783.
35. Vry, JD, Martínez-Martínez, P, Losen, M, Bode, GH, Temel, Y, Steckler, T, et al. (2010). Low current driven micro-electroporation allows efficient in vivo delivery of nonviral DNA into the adult mouse brain. *Mol Ther* **18**: 1186–1191.
36. Fujimoto, H, Kato, K and Iwata, H (2008). Electroporation microarray for parallel transfer of small interfering RNA into mammalian cells. *Anal Bioanal Chem* **392**: 1309–1316.
37. Yamauchi, F, Kato, K and Iwata, H (2005). Layer-by-layer assembly of poly(ethyleneimine) and plasmid DNA onto transparent indium-tin oxide electrodes for temporally and spatially specific gene transfer. *Langmuir* **21**: 8360–8367.
38. Kawano, T, Yamagata, M, Takahashi, H, Niidome, Y, Yamada, S, Katayama, Y et al. (2006). Stabilizing of plasmid DNA in vivo by PEG-modified cationic gold nanoparticles and the gene expression assisted with electrical pulses. *J Control Release* **111**: 382–389.
39. Ovcharenko, D, Jarvis, R, Hunicke-Smith, S, Kelnar, K and Brown, D (2005). High-throughput RNAi screening in vitro: from cell lines to primary cells. *RNA* **11**: 985–993.
40. Ziauddin, J and Sabatini, DM (2001). Microarrays of cells expressing defined cDNAs. *Nature* **411**: 107–110.
41. Doyle, SR and Chan, CK (2007). Differential intracellular distribution of DNA complexed with polyethylenimine (PEI) and PEI-polyarginine PTD influences exogenous gene expression within live COS-7 cells. *Genet Vaccines Ther* **5**: 11.
42. Lin, R, Chang, DC and Lee, YK (2011). Single-cell electroendocytosis on a micro chip using in situ fluorescence microscopy. *Biomed Microdevices* **13**: 1063–1073.
43. Antov, Y, Barbul, A, Mantsur, H and Korenstein, R (2005). Electroendocytosis: exposure of cells to pulsed low electric fields enhances adsorption and uptake of macromolecules. *Biophys J* **88**: 2206–2223.
44. Faurie, C, Phez, E, Golzio, M, Vossen, C, Lesbordes, JC, Delteil, C et al. (2004). Effect of electric field vectoriality on electrically mediated gene delivery in mammalian cells. *Biochim Biophys Acta* **1665**: 92–100.
45. Tomov, TC and Tsoneva, IC (1989). Changes in the surface charge of cells induced by electrical pulses. *Bioelectroch Bioener* **22**: 127–133.
46. Nagahara, AH, Merrill, DA, Coppola, G, Tsukada, S, Schroeder, BE, Shaked, GM et al. (2009). Neuroprotective effects of brain-derived neurotrophic factor in rodent and primate models of Alzheimer's disease. *Nat Med* **15**: 331–337.
47. Hamamichi, S, Rivas, RN, Knight, AL, Cao, S, Caldwell, KA and Caldwell, GA (2008). Hypothesis-based RNAi screening identifies neuroprotective genes in a Parkinson's disease model. *Proc Natl Acad Sci USA* **105**: 728–733.
48. Brijbassi, S, Amtul, Z, Newbigging, S, Westaway, D, St George-Hyslop, P and Rozmahel, RF (2007). Excess of nicastrin in brain results in heterozygosity having no effect on endogenous APP processing and amyloid peptide levels in vivo. *Neurobiol Dis* **25**: 291–296.
49. Corder, EH, Saunders, AM, Strittmatter, WJ, Schmechel, DE, Gaskell, PC, Small, GW et al. (1993). Gene dose of apolipoprotein E type 4 allele and the risk of Alzheimer's disease in late onset families. *Science* **261**: 921–923.
50. Engelborghs, S, Dermaut, B, Mariën, P, Symons, A, Vloeberghs, E, Maertens, K et al. (2006). Dose dependent effect of APOE epsilon4 on behavioral symptoms in frontal lobe dementia. *Neurobiol Aging* **27**: 285–292.
51. Combarros, O, Sánchez-Guerra, M, Infante, J, Llorca, J and Berciano, J (2002). Gene dose-dependent association of interleukin-1A [-889] allele 2 polymorphism with Alzheimer's disease. *J Neurol* **249**: 1242–1245.

Supplementary Information accompanies this paper on the Molecular Therapy–Nucleic Acids website (http://www.nature.com/mtna)